Preparation of Ultrahigh-Molecular-Weight Polyethylene/Carbon Nanotube Nanocomposites with a Ziegler–Natta Catalytic System and Investigation of Their Thermal and Mechanical Properties

B. Meschi Amoli,[1] S. A. Ahmad Ramazani,[1] Hadi Izadi[2]

[1]*Polymer Group, Department of Chemical and Petroleum Engineering, Sharif University of Technology, Tehran, Iran*
[2]*Chemical Engineering Department, University of Waterloo, Waterloo, ON, Canada, N2L 3G1*

Received 10 June 2010; accepted 14 October 2011
DOI 10.1002/app.36368
Published online 28 January 2012 in Wiley Online Library (wileyonlinelibrary.com).

ABSTRACT: In this research, ultrahigh-molecular-weight polyethylene (UHMWPE)/multiwalled carbon nanotube (MWCNT) nanocomposites with different nanotube concentrations (0.5, 1.5, 2.5, and 3.5 wt %) were prepared via *in situ* polymerization with a novel, bisupported Ziegler–Natta catalytic system. Magnesium ethoxide [$Mg(OEt)_2$] and surface-functionalized MWCNTs were used as the support of the catalyst. Titanium tetrachloride ($TiCl_4$) accompanied by triethylaluminum constituted the Ziegler–Natta catalytic system. Preparation of the catalyst and the polymerization were carried out in the slurry phase under an argon atmosphere. Support of the catalyst on the MWCNTs was investigated with Fourier transform infrared spectroscopy. The results confirmed the interaction between the catalyst and the MWCNT hydroxyl groups. Intrinsic viscosity measurements showed an ultrahigh molecular weight in the produced samples. Scanning electron microscopy images confirmed the good dispersion of MWCNTs throughout the polyethylene (PE) matrix. The crystallization behavior of the samples was examined with differential scanning calorimetry. Its results showed that the crystal content of the samples increased with increasing MWCNT concentration up to 1.5 wt %. The same trend was observed for the crystallization temperature, whereas the melting temperature did not change with increasing MWCNT concentration up to 1.5 wt %, but it decreased beyond this concentration. In addition, thermogravimetric analysis results showed that the addition of MWCNTs noticeably improved all of the investigated thermal stability factors of the UHMWPE/MWCNT nanocomposites compared to those of pure PE. The results obtained from tensile testing revealed significant increases in the Young's modulus, yield stress, and ultimate tensile strength. This indicated a tremendous improvement in the mechanical properties of the PE/MWCNT nanocomposites compared to those of pure PE. J Appl Polym Sci 125: E453–E461, 2012

Key words: carbon nanotubes; nanocomposites; polyethylene (PE); Ziegler–Natta polymerization

INTRODUCTION

Nowadays, polyethylene (PE), because of its low cost, low density, high electrical resistance, nontoxicity, and easy processability, is known as one of the most widely used polymers in nanocomposite production.[1,2] During recent decades, many efforts have been devoted to the manufacture of different types of PE nanocomposites with nanosized fillers, specifically carbon nanotubes (CNTs). CNTs, because of their high aspect ratio and exceptional electrical and mechanical properties, have been considered interesting reinforcing fillers for the fabrication of high-performance polymeric nanocomposites. Therefore, the manufacturing and investigation of the properties of PE/CNT nanocomposites have captured lots of attention.[3–9] However, the uniform dispersion of CNTs throughout the PE matrix, specifically ultrahigh-molecular-weight polyethylene (UHMWPE), is one of the most challenging concerns in this approach. Physical blending methods, such as melt and solution mixing, which are conventional methods for the preparation of most CNT nanocomposites, usually lead to the poor dispersion of fillers throughout the matrix. Also, because of the lack of flow and the solubility of UHMWPE, the production of its nanocomposites by these conventional methods encounters many technical difficulties.

In situ polymerization, as an alternative method that can overcome the CNT limited dispersity in different polymers, has been extremely developed.[10–15] *In situ polymerization* refers to a method in which the polymerization and the filler loading are carried out simultaneously. In this method, the polymerization takes place on the filler surface; this can, consequently, reduce the filler agglomeration by reducing

Correspondence to: S. A. A. Ramazani (ramazani@sharif.edu).

the affinity of the filler particles to each other. Generally, although a large body of literature has been devoted to the study and improvement of the dispersion of CNTs throughout the polymer matrix,[16–20] few have investigated the capability of *in situ* polymerization for this purpose. For instance, Trujillo et al.[14] and Kaminsky et al.[15] manufactured PE/multiwalled carbon nanotube (MWCNT) nanocomposites via *in situ* polymerization with metallocene catalysts. In their works, they investigated the crystallization behavior and the primary mechanical properties of their samples. Bredeau et al.[21] generated high-performance polyolefinic nanocomposites by ethylene–norbornene copolymerization using a CNT-supported metallocene catalyst. Recently, Ramazani et al.[10] developed a new, bisupporting method for the *in situ* preparation of polyolefinic nanocomposites. This approach was applied to the synthesis of different nanocomposites, such as PE/nanoclay[10,12] and polypropylene/nanoclay,[11,13] and led to production of fully exfoliated nanoclay structures. An analysis of the thermal and the mechanical properties of these nanocomposites showed great improvement in these properties compared to nanoclay composites fabricated by conventional methods, such as physical blending. On the other hand, from an industrial point of view, the *in situ* polymerization method can be a cost-effective candidate for the mass production of PE nanocomposites; for instance, nanocomposites can be produced in a plant of high-density PE (e.g., loop reactors) without any considerable modification in the plant. All in all, *in situ* polymerization can be considered as an efficient and cost-effective method for the production of PE/CNT nanocomposites with a uniform dispersion of CNTs in the PE matrix, and it can also improve the interactions between the nanotubes and the polymeric chains.

However, although polyolefinic nanocomposites have been studied in recent years, few efforts have been devoted to the production of ultrahigh-molecular-weight polyolefinic nanocomposites with CNTs. Kaminsky and Funck[22] produced UHMWPE/MWCNT and ultrahigh-molecular-weight polypropylene/MWCNT nanocomposites using metallocene via *in situ* polymerization. In their work, they investigated the influence of the nanotube concentration on the thermal characteristics of their products. However, they did not report the exact molecular weight of their product. In another study, Sanchez et al.[23] produced UHMWPE/MWCNT nanocomposites using *in situ* polymerization by a $TpTiCl_2(Et)$ system. They investigated the effects of the CNT concentration on the activation of the catalyst. With respect to thermogravimetric analysis (TGA) results, they reported that the thermal stability of the samples did not change, whereas the differential scanning calorimetry (DSC) results showed a slight increase in the crystallinity of their products. Park and Choi[24] also reported a novel method using a metallocene-based (i.e., half-titanocene) catalyst for the production of UHMWPE/MWCNT nanocomposites; they also did not report the exact molecular weight of their product because of technical difficulties.

Even though the previously reported works on the preparation of UHMWPE/MWCNT nanocomposites used metallocene catalyst systems, in this report, the preparation of UHMWPE/MWCNT nanocomposites via *in situ* polymerization with a bisupported Ziegler–Natta catalytic system is introduced for the first time. It is worthwhile to mention that the Ziegler–Natta catalyst systems are less sensitive to impurities and also less expensive compared to metallocene-based systems. In addition, the mechanical properties of UHMWPE/MWCNT nanocomposites (hereafter referred to as PE/MWCNT), which have not been systematically investigated yet, are reported along with the other physical properties of the samples.

EXPERIMENTAL

Materials

Hydroxyl-functionalized MWCNTs (OH content = 3.06 wt %) with inner diameters of 5–10 nm and outer diameters of 10–20 nm (grade TNM3) were supplied by Chengdu Organic Chemicals Co., Ltd. (Timesnano, Chengdu, China). According to the specifications from the supplier, these MWCNTs were produced by natural-gas catalytic decomposition over a Ni-based catalyst, and OH functionalization was carried out via $KMnO_4$ oxidation in an HCl solution. The size of the nanotubes was measured with high-resolution transmission electron microscopy, and the OH content was also characterized with X-ray photoelectron spectroscopy and volumetric estimation. We further purified the ethylene monomer (industrial grade), which was supplied by Amir Kabir Petrochemical Co., by passing the monomer through molecular sieve columns (4A type having a 4-Å pore size). High-purity argon (99.999%) was used to produce an inert atmosphere in the catalyst preparation and the polymerization processes. Industrial-grade *n*-hexane from Amir Kabir Petrochemical Co. was further dried by a sodium benzophenone complex (diphenyl ketyl). Titanium tetrachloride ($TiCl_4$; $\geq$99%, Riedel-de Haen Chemical Laboratory) was used as the catalyst. Magnesium ethoxide [$Mg(OEt)_2$; $\geq$95%, Fluka] and dibutyl phthalate (as an internal donor, Merck KGaA) were used for the preparation of the catalyst. Triethylaluminum ($AlEt_3$; $\sim$ 15% in hexane, Fluka) was used as the cocatalyst. All other chemicals and solvents were

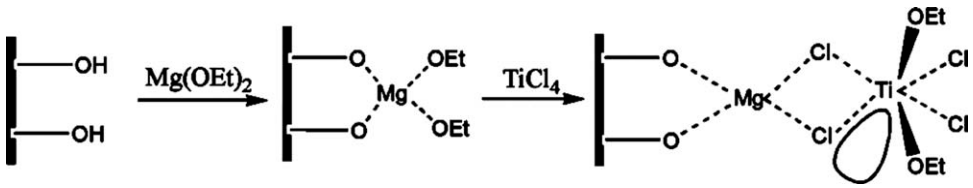

Figure 1 Schematic of the mechanism of the supporting Ziegler–Natta catalyst on the MWCNTs in the presence of $Mg(OEt)_2$.

purchased with the highest purity and were used as received without further purification.

Catalyst preparation

The catalyst preparation was carried out according to our previous studies with some modifications.[10–13] To dry the MWCNTs, they were heated for 2 h at 200°C *in vacuo*. In a glovebox, 8 g of the calcinated MWCNTs and $Mg(OEt)_2$ (4 : 1 weight fraction) were fed into a triple-necked, round-bottom flask as the catalyst preparation reactor. The flask was equipped with a magnetic stirrer and was immersed in an oil bath. Because the reaction needed to be carried out in an inert atmosphere, the flask was sealed, degassed, and backfilled with high-purity argon. Two flask openings were equipped with gas valves, and the third was sealed with a rubber septum. Degassing and backfilling with argon was carried out three times to assure completely inert conditions. Then, 150 mL of *n*-hexane/toluene (50/50 wt %) was injected into the reactor, and the temperature was gradually increased to 80°C while the flask contents were vigorously stirred. Subsequently, 8 mL of $TiCl_4$ and 1 mL of dibutyl phthalate were added to the mixture, and the flask contents were stirred for 2 h at 80°C. The final product was washed with *n*-hexane at 50°C under an argon atmosphere. Washing was carried out 10 times to assure the complete removal of the unreacted residuals from MWCNT–catalyst complex. Then, the MWCNT–catalyst complex was dissolved in 100 mL of *n*-hexane for its future application in polymerization.

Figure 1 shows the schematic of the mechanism of the supporting Ziegler–Natta catalyst on the MWCNTs in the presence of $Mg(OEt)_2$. Samples taken from the flask for characterization were dried *in vacuo* at 70°C. Fourier transform infrared (FTIR) spectroscopy was applied to confirm the interaction between the MWCNTs and $Mg(OEt)_2$. The spectra were measured with a Horiba FT-210 infrared spectrometer (Horiba, Ltd., Kyoto, Japan) with a 150-mg KBr disk (0.4 wt % fixed solid content), whereas the background was tuned by a blank KBr pellet. The FTIR spectrum of the hydroxyl-functionalized MWCNTs [Fig. 2(a)] exerted two characteristic peaks at 3148 and 3425 cm^{-1}, which indicated the existence of two types of hydroxyl groups at the nanotube surface. The first peak was due to the existence of conjugate hydroxyl groups, whereas the second confirmed the presence of nonconjugate hydroxyl groups at the MWCNT surface. On the other hand, in Figure 2(b), which shows the spectrum of the supported catalyst, it can be observed that the size of the peak related to the conjugate hydroxyl groups was significantly reduced, whereas the peak related to the nonconjugate hydroxyl groups still remained unchanged. So, we concluded that the catalyst should have formed a complex with only conjugate hydroxyl groups; this is schematically represented in Figure 3.

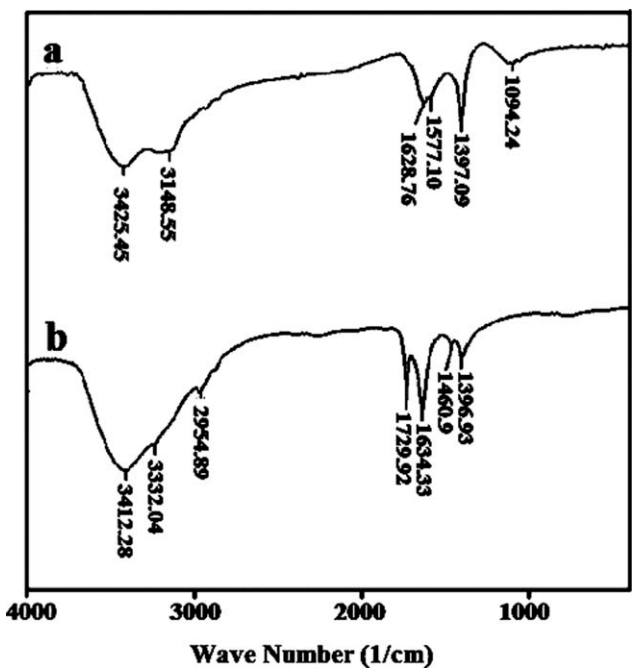

Figure 2 FTIR spectra of the (a) hydroxyl-functionalized MWCNTs and (b) MWCNT–catalyst complex.

Figure 3 Schematic of the $Mg(OEt)_2$ complex formation with conjugate hydroxyl groups on the MWCNT surface.

In situ polymerization

The polymerization procedure was adopted from our previous studies with appropriate modifications.[10–13] The polymerization was carried out in the slurry phase in a pressure reactor (1 L, versoclave, Büchi AG) equipped with a mechanical stirrer and a temperature- and pressure-control system. First, the reactor was sealed, degassed, and backfilled with high-purity argon. After three degassing and backfilling procedures, the reactor was purged for 1 h with argon at 1.1 bar. Then, 500 mL of degassed *n*-hexane was transferred to the reactor with cannula transfer; during stirring, 10 mL of degassed triethylaluminum (10 vol % in *n*-hexane) was injected into the reactor, and after 5 min, 10 mL of the MWCNT–catalyst complex was injected. Immediately, ethylene monomer was introduced into the reactor at 7 bar, and polymerization was carried out for the desired time. Generally, to achieve different MWCNT weight fractions, two approaches could be followed. In the first approach, different amounts of the MWCNT–catalyst complex could be added to the reactor while the polymerization duration was kept constant. In the second approach, the polymerization time could be changed while a constant amount of MWCNT–catalyst complex was used. In this study, we produced nanocomposites with different MWCNT weight fractions by changing the polymerization duration. In the end, to terminate the polymerization, the ethylene inlet was closed, the reactor was purged with air, and HCl was injected into the reactor to make sure that the catalyst was deactivated. Finally, after the reactor temperature was brought down to room temperature, the nanocomposites were removed from the reactor, vacuum-filtered, washed with ethanol and acetone, and dried *in vacuo* at 70°C for 24 h. The synthesis of pure PE, as the reference, was carried out under the same conditions under which the nanocomposites were produced, except that MWCNT was not used in the catalyst system.

Characterization

The morphology and degree of dispersion of the MWCNTs in the PE matrix were characterized by scanning electron microscopy (SEM). With a Tescan VEGA SEM instrument (Tescan USA, Inc.) at an operating voltage of 15 kV, SEM images were taken from the fracture surface of the nanocomposite films, which were fabricated by hot pressing.[25] Samples were broken in liquid nitrogen, and images were taken from different zones of the fracture surface.[25] In addition, energy-dispersive X-ray spectroscopy (EDX) was performed to analyze the MWCNT distribution throughout the matrix. To characterize the molecular weight of the prepared nanocomposites, the viscosity-average molecular weights (M_V's) of all of the samples were measured. The measurement was carried out with an Ubbelohde suspended level dilution viscometer. The melting temperature (T_m), crystallization temperature (T_c), heat of fusion, and content of crystallinity of the samples were measured by DSC with a Pyris 1 DSC calorimeter (PerkinElmer, Inc.) under a nitrogen atmosphere. Initially, the samples were heated from 40 to 200°C at a constant rate of 10°C/min. They were held at 200°C for 3 min to eliminate their thermal history. Subsequently, they were cooled down to 40°C at the same rate. They were held at that temperature for 1 min before they were again heated to 200°C. The thermal stability of nanocomposites was investigated by TGA according to ASTM E 1131-03 with a PL-1500 instrument (Polymer Laboratories). We carried out TGA by heating 2.5-mg samples from 50 to 650°C at a rate of 10°C/min under a nitrogen atmosphere. The mechanical properties of the samples, including their Young's modulus, yield stress, and tensile strength, were measured by tensile testing according to ASTM D 882-02. For each sample, five sheets with dimensions of $10 \times 1 \times 0.5$ cm^3 (Length × Width × Thickness), which were fabricated by hot pressing, were characterized at ambient temperature (the tensile speed was set at 5 mm/min). Dynamic mechanical thermal analysis (DMTA) of samples was performed with a dynamic mechanical analyzer (Tritec 2000 DMA) from Triton Technology, Ltd., according to ASTM E 1640-04. The applied strain was 0.02%, whereas the frequency was set at 1 Hz. The temperature range was −150 to 300°C, and the temperature was increased at a constant rate of 10°C/min. The size (Length × Width × Thickness) of the samples was $5 \times 3 \times 0.3$ cm^3.

RESULTS AND DISCUSSION

Morphological study

As previously mentioned, the dispersion and distribution of the MWCNTs in the PE matrix are crucial parameters that can affect the thermal and mechanical performance of fabricated nanocomposites. Figure 4(a,b) shows the SEM images obtained from the fracture surfaces of the PE/MWCNT nanocomposites containing 1.5 and 3.5 wt % MWCNTs, respectively. Although no filler agglomeration was observed for any of the samples, nanotubes in the 3.5 wt % sample [Fig. 4(b)] were much closer to each other compared to those in the 1.5 wt % sample [Fig. 4(a)]. The distribution of the MWCNTs was studied with EDX maps. Figure 5(a,b) represents the EDX maps of chlorine and titanium, respectively, for the 1.5 wt % PE/MWCNT nanocomposite. These maps show the homogeneous dispersion of the

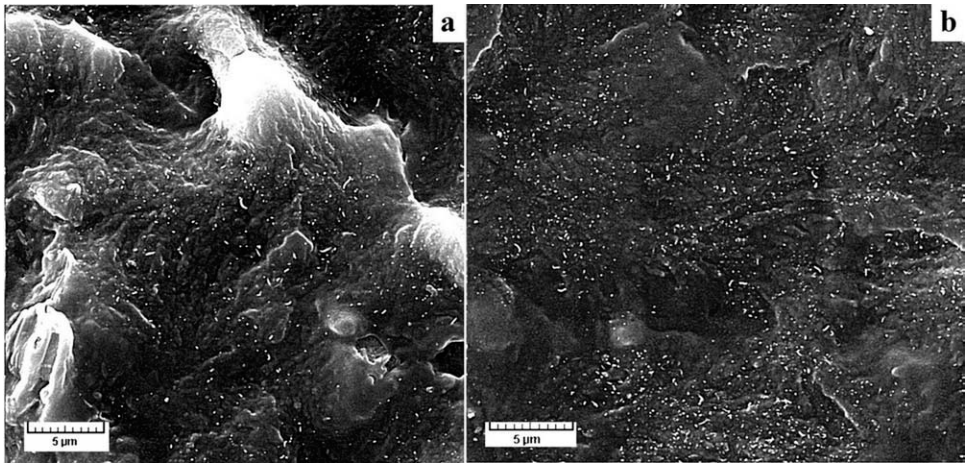

Figure 4 SEM images of the fracture surfaces of the PE/MWCNT nanocomposites: (a) 1.5 and (b) 3.5 wt % MWCNTs.

catalyst throughout the matrix. With the knowledge that the catalyst was supported on nanotubes, these images could be considered as an indirect evidence of the homogeneous distribution of nanotubes throughout the polymeric matrix.

Molecular weight investigation

Because of the presence of nanotubes in the produced nanocomposites and also the ultrahigh-molecular-weight of the polymer, the determination of the nanocomposites' molecular weights with conventional characterization methods, which are mostly based on size-exclusion chromatography or light scattering techniques, was not practical and precise for our system.[22,24] Therefore, the viscosity–molecular weight relationship was used to investigate the M_V values of the nanocomposites and the pure PE (Table I). For this purpose, samples were dissolved in xylene at 135°C and then transferred to the viscometer immersed in an oil bath at the same temperature. With the Mark–Houwink Sakurada equation, the intrinsic viscosity ([η]) could be used to calculate M_V by $[\eta] = KM_V^{\alpha}$, where K (6.77×10^{-4} dL/g) and α (0.67) are Mark–Houwink constants.[26] The obtained results for the molecular weight were comparable to those previously reported in the literature.[23] Although the molecular weight of samples increased with increasing MWCNT concentration (up to 1.5 wt %), beyond this concentration, it decreased with increasing MWCNT content (Table I).

Crystallization and structural characteristics

T_m and T_c of the PE and PE/MWCNT nanocomposites were determined with DSC. As can be seen in Figure 6 and Table II, T_m of the nanocomposites did not change (within the experimental error) as the MWCNT content increased up to 1.5 wt %, but beyond this concentration, it decreased slightly. This was an expected behavior, in that MWCNTs act as an impurity in PE during its crystallization. In other

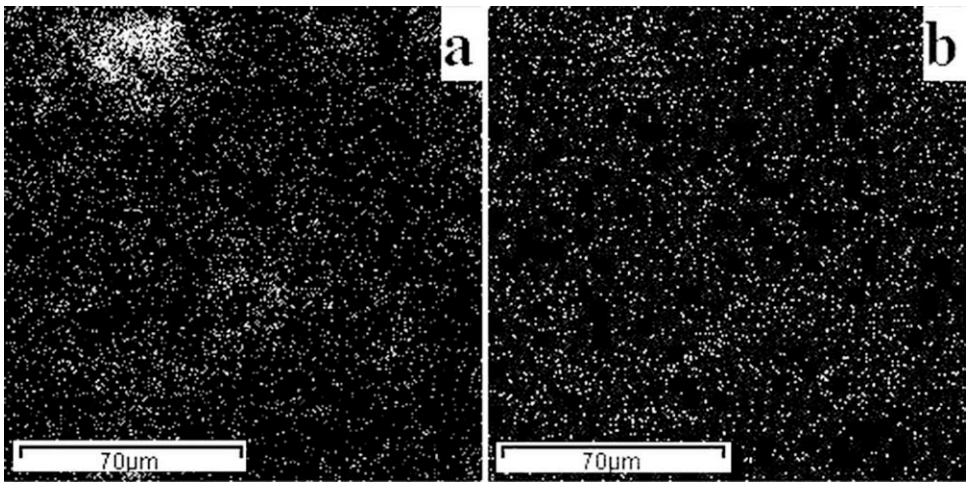

Figure 5 EDX maps of (a) chlorine and (b) titanium for the PE/MWCNT nanocomposites containing 1.5 wt % MWCNTs.

TABLE I
Molecular Weights (MWs) of the PE and PE/MWCNT Nanocomposites

MWCNT concentration (wt %)	MW (g/mol)
0	2.8×10^6
0.5	2.9×10^6
1.5	3.2×10^6
2.5	2.8×10^6
3.5	2.6×10^6

TABLE II
DSC Results for the PE and PE/MWCNT Nanocomposites

MWCNT concentration (wt %)	T_m (°C)	T_c (°C)	ΔH_f (kJ/kg)	X (%)
0	140	116	84.3	28
0.5	140	118	109.3	37
1.5	140	120	117.5	40
2.5	139	119	114.9	39
3.5	136	117	100.3	34

words, although a low concentration did not affect the nanocomposites' T_m's, enhanced concentrations decreased T_m. On the other hand, T_c values of the nanocomposites increased with increasing MWCNT concentration up to 1.5 wt % and then decreased beyond this concentration (Fig. 7). Furthermore, the percentage crystallinity (X; %) of the pure PE and PE/MWCNT nanocomposites was calculated by

$$X(\%) = \left(\frac{\Delta H_f}{\Delta H_f^o}\right) \times 100\%$$

where ΔH_f is the heat of fusion of the nanocomposites as determined by DSC and ΔH_f^o is the heat of fusion of pure PE (293 J/g).[17] X versus MWCNT concentration showed the same trend as T_c (Table II).

All in all, according to Table II, which summarizes the T_m, T_c, heat of fusion, and content of crystallinity values for both the pure PE and PE/MWCNT nanocomposites, we observed that the addition of MWCNTs up to 1.5 wt % slightly increased the content of crystallinity. Generally, the addition of solid particles (impurities) to a polymer matrix can induce the content of crystallinity because of the heterogeneous nucleation of crystalline microdomains.[14,22,23] However, enhanced amounts of particles can hinder the content of crystallinity because they add more defects to the polymer matrix crystals, which consequently reduces the density of the unit cells.[14] In other words, the hindered segmental movements of PE chains due to limited accessible volume to crystalline microdomains reduced the content of crystallinity for nanocomposites containing more than 1.5 wt % MWCNTs.

TGA

Figure 8 represents the nonisothermal degradation characteristics of the PE and PE/MWCNT nanocomposites. Extracted data from Figure 8 are presented in Table III, in which $T_{0.1}$ and $T_{0.5}$ represent the onset degradation temperature and the midpoint degradation temperature, respectively. In contrast to data presented by Sanchez et al.,[23] we observed that the MWCNT incorporation in the PE matrix, even at the minimum concentration (0.5 wt %), increased $T_{0.1}$ up to 18°C compared to that in the pure PE sample. Small amounts of MWCNTs also increased $T_{0.5}$ and the ash content of the nanocomposite significantly. However, higher concentrations of MWCNTs (up to 2.5 wt %) did not affect $T_{0.1}$ and $T_{0.5}$

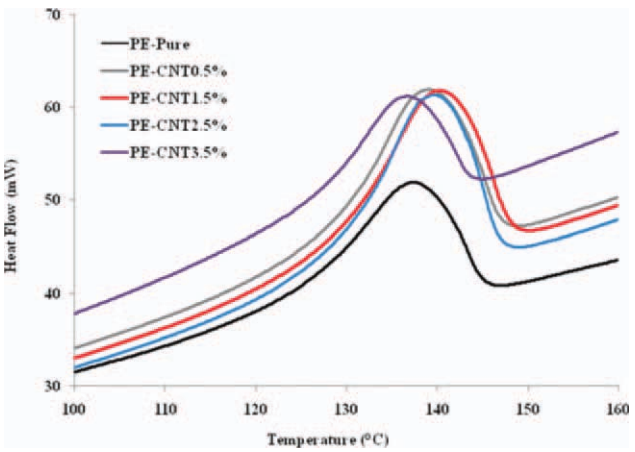

Figure 6 DSC heating scan of the PE and PE/MWCNT nanocomposites. [Color figure can be viewed in the online issue, which is available at wileyonlinelibrary.com.]

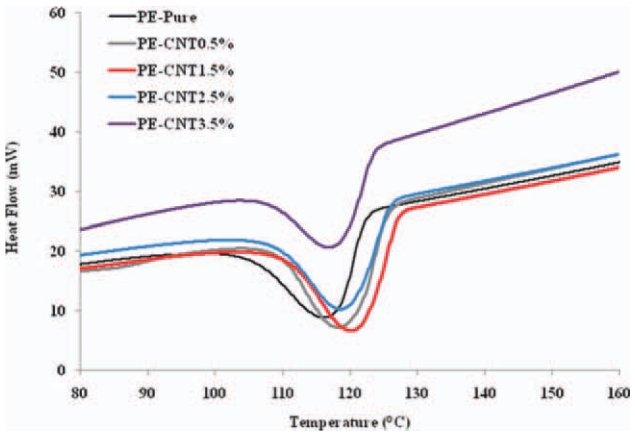

Figure 7 DSC cooling scan of the PE and PE/MWCNT nanocomposites. [Color figure can be viewed in the online issue, which is available at wileyonlinelibrary.com.]

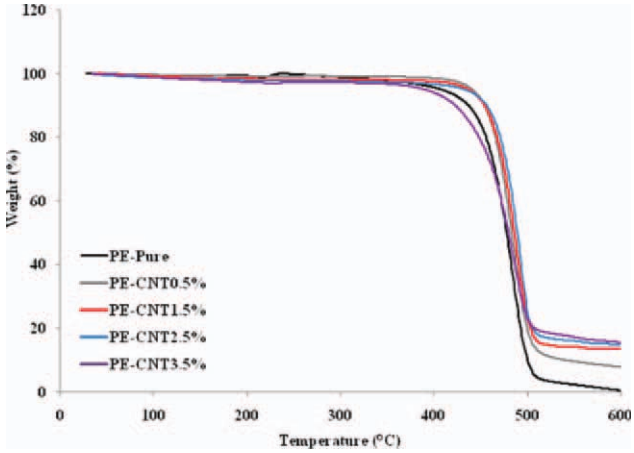

Figure 8 Weight loss versus temperature in the nonisothermal degradation of the PE and PE/MWCNT nanocomposites. [Color figure can be viewed in the online issue, which is available at wileyonlinelibrary.com.]

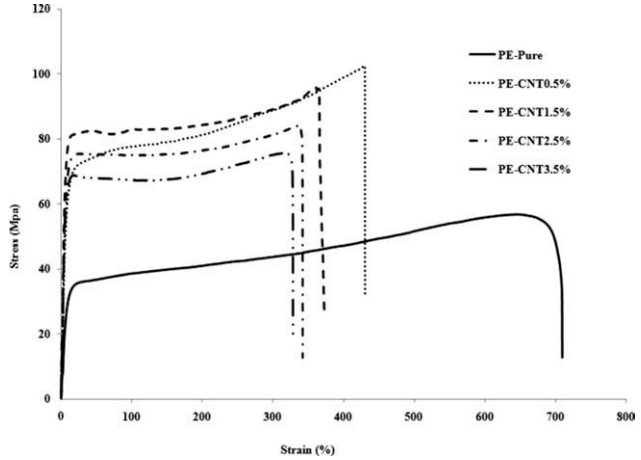

Figure 9 Stress versus strain for the PE and PE/MWCNT nanocomposites.

significantly, whereas the ash residue increased with increasing MWCNT concentration in the nanocomposite. It seemed that the introduction of MWCNTs into the PE matrix (up to 2.5 wt %) retarded the thermal decomposition of the PE nanocomposites. This effect was attributed to the barrier effect of the CNTs, which prevented the transport of volatile gases through the nanocomposite.[27] However, the nanocomposite with 3.5 wt % MWCNTs experienced smaller $T_{0.1}$ and $T_{0.5}$ values compared to the nanocomposites with lower MWCNT contents. Because the 3.5 wt % sample had the highest ash content, we concluded that the formation of contact between the CNTs and, consequently, more localized PE zones in the nanocomposite at high nanotube concentrations must have been the source of the lower decomposition temperatures (i.e., $T_{0.1}$ and $T_{0.5}$). However, it should be noted that the thermal stability of the 3.5 wt % sample was still improved compared to that of pure PE.

Mechanical properties

Figure 9 represents typical stress–strain curves of the PE and PE/MWCNT nanocomposites. It was observed that the addition of even small amounts of MWCNTs into the PE matrix significantly improved the mechanical properties of PE. The changes in the mechanical properties, including the Young's modulus, yield stress, and tensile strength, which were extracted from Figure 9, are presented in Figures 10–12. The introduction of MWCNTs (up to 1.5 wt %) enhanced the Young's modulus of the nanocomposites (~ 100%) compared to that of pure PE (Fig. 10). However, at higher concentrations (i.e., higher than 1.5 wt %), the Young's modulus of the nanocomposites decreased slightly compared to that of the 1.5 wt % sample, whereas it was still much higher than that of pure PE. Although the addition of filler generally can improve the Young's modulus of polymers, the huge elevation in the Young's modulus of this system was due to the extremely high modulus of the CNTs, which was approximately four orders of magnitude higher than that of pure PE. However, one should bear in mind that the *in situ*

TABLE III
TGA Results for the PE and PE/MWCNT Nanocomposites

MWCNT concentration (wt %)	$T_{0.1}$ (°C)	$T_{0.5}$ (°C)	Ash content (wt %)
0	436	477	0.3
0.5	454	483	7.7
1.5	454	486	13.5
2.5	456	490	14.5
3.5	423	479	15.4

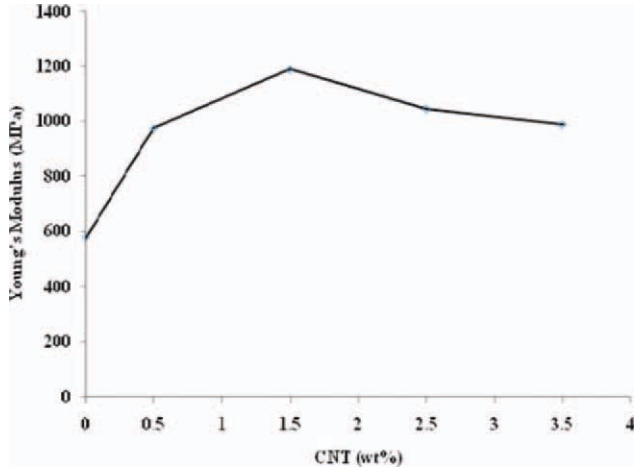

Figure 10 Young's moduli of the pure PE and PE/MWCNT nanocomposites at different concentrations.

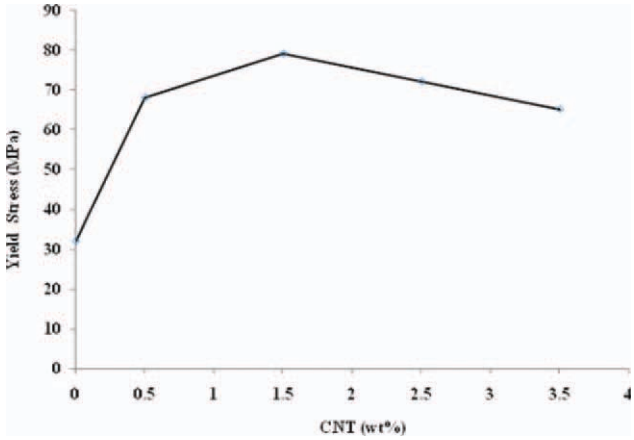

Figure 11 Yield stress of the pure PE and PE/MWCNT nanocomposites at different concentrations.

polymerization of PE enabled the improved dispersion of MWCNTs and also more efficient joints between the polymer and the filler, which consequently improved the transfer of load throughout the matrix.

The yield stress results, as the second mechanical property of the PE/MWCNT nanocomposites that was investigated in this study, also showed the same trend as the Young's modulus results (Fig. 11); the yield stress of the 1.5 wt % sample was about 1.5 times higher than that of pure PE, whereas the yield stress decreased slightly with addition of higher amounts of MWCNTs beyond 1.5 wt %. Because the trend of changes in the crystal content of the nanocomposites was the same as the yield stress changes, we concluded that the crystal dislocation could not have been the influential factor on the yield stress improvement. However, although a comparison of the yield stress changed trend with the nanocomposite molecular weight, the effect of the polymer's molecular weight on the plastic deformation at amorphous regions of the polymer was more elaborate. Generally, an increase in the molecular weight results in a lower number of chain ends in a unit volume of a nanocomposite; higher numbers of chain ends in the bulk and, therefore, a higher free volume in the nanocomposite matrix caused easier plastic deformation of the samples, in that the free volume acted as wasted space in the polymer matrix. The last but not the least was the investigation of the effect of the MWCNTs on the tensile strength, as presented in Figure 12. With the addition of only 0.5 wt % MWCNTs to the PE matrix, a great increase in the tensile strength of the samples was observed, whereas the addition of more MWCNTs gradually decreased the tensile stress. Although the tensile stress of the nanocomposites decreased beyond this concentration, it was still much higher than that of pure PE.

The storage modulus (E'), which characterizes the stored energy representing the elastic portion of a viscoelastic material, was measured by DMTA (Fig. 13). It should be noted that the DMTA result for the 1.5 wt % sample was not plotted because of its inconsistency during the test. The specific properties of this sample, as observed in almost all of the characterization results, must have been the source of this unknown inadaptability of the sample with DMTA. The data extracted from Figure 13 at room temperature completely confirmed the results from the tensile tests. However, above the T_m, it was observed that E' increased and showed a peak. Although the temperature was well above the glass-transition temperature of the polymer (Fig. 14), because of the high molecular weight of the polymer, the relaxation time for the polymer chains must

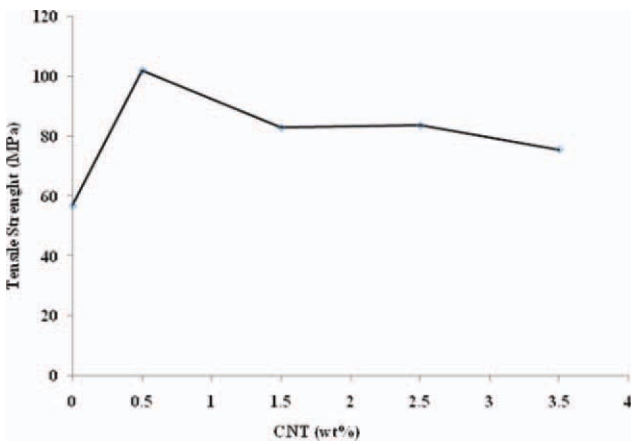

Figure 12 Tensile strength of the pure PE and PE/MWCNT nanocomposites at different concentrations.

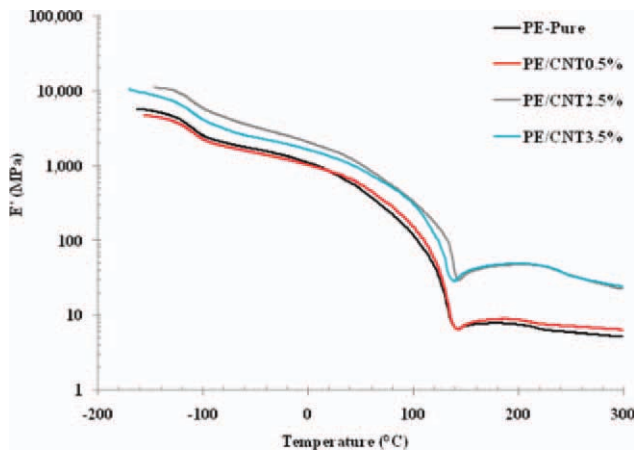

Figure 13 E' versus temperature for the PE and PE/MWCNT nanocomposites. [Color figure can be viewed in the online issue, which is available at wileyonlinelibrary.com.]

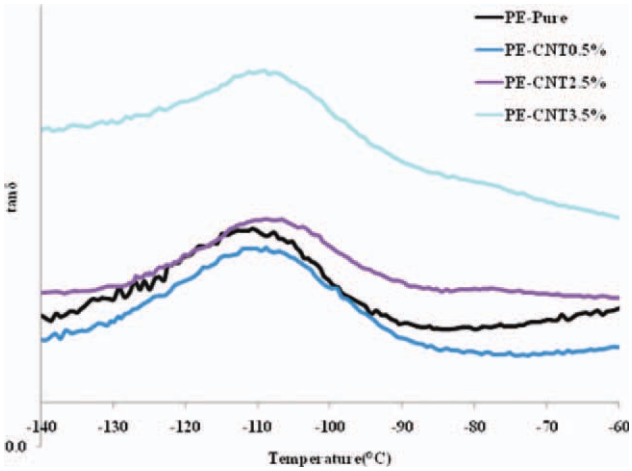

Figure 14 Phase angle (tan δ = Loss modulus/E') versus temperature for the PE and PE/MWCNT nanocomposites. [Color figure can be viewed in the online issue, which is available at wileyonlinelibrary.com.]

have been higher than the timescale of the experiment, which yielded an increase in E' of the polymer after T_m.

All in all, the better dispersion of dispersed phase, due to the polymerization technique used, and the higher interphase surface area resulted in the surprisingly improved mechanical properties of the produced nanocomposites compared to those of the pure PE. Surely, this was indicative that the best dispersion and distribution could only be attained at lower MWCNT loadings. At high nanotubes loadings, it seemed that because of the tendency of the nanotubes to agglomerate and some physical contacts between them, the load transfer from the PE matrix to the nanotubes could be effectively carried out; this resulted in a slight reduction in the mechanical and thermophysical properties of the nanocomposites. So, it seemed that the best dispersions of the nanotubes in the PE matrix and so the best mechanical and thermophysical properties could be attained at low nanotube loadings, specifically at 1.5 wt % in this study.

CONCLUSIONS

In this research, UHMWPE/MWCNT nanocomposites were produced via *in situ* polymerization with a novel Ziegler–Natta catalytic system. The catalyst was grafted to the surface of the MWCNTs, and the *in situ* polymerization was initiated from MWCNTs' surface. This novel approach for the fabrication of UHMWPE/MWCNT nanocomposites resulted in the improved dispersion and distribution of MWCNTs throughout the polymer matrix. This, consequently, improved the thermal and mechanical properties of the fabricated nanocomposites. On the basis of the characterization results, we observed that the thermal properties were dramatically improved compared to those of pure UHMWPE. On the other hand, a significant improvement in the mechanical properties, even at low concentrations of MWCNTs, indicated efficient interaction between the MWCNTs and PE chains.

References

1. Kuran, W. Principles of Coordination Polymerization; Wiley: New York, 2001.
2. Lee, D.; Kim, H.; Yoon, K.; Min, K. E.; Seo, K. H.; Noh, S. K. Sci Technol Adv Mater 2005, 6, 457.
3. Steinmetz, J.; Lee, H.; Kwon, S.; Lee, D.; Bac, C. G.; Hamad, E. A.; Kim, H.; Park, Y. Curr Appl Phys 2007, 7, 39.
4. Slobodian, P.; Pavlinek, V. Curr Appl Phys 2009, 9, 184.
5. Tong, X.; Liu, C.; Cheng, H.; Zhao, H.; Yang, F.; Zhang, X. Appl Polym Sci 2003, 92, 3697.
6. Bocchini, S.; Frache, A.; Camino, G.; Claes, M. Eur Polym J 2007, 43, 3222.
7. McNally, T.; Potschke, P.; Halley, P.; Murphy, M.; Martin, D.; Bell, S. E. J.; Brennan, G. P.; Bein, D.; Lemoine, P.; Quinn, J. P. Polymer 2005, 46, 8222.
8. Valentini, L.; Armentano, I.; Biagiotti, J.; Frulloni, E.; Kenny, J. M.; Santucci, S. Diamond Relat Mater 2003, 12, 1601.
9. Xiong, J.; Zheng, Z.; Qin, X.; Li, M.; Li, H.; Wang, X. Carbon 2006, 44, 2701.
10. Ramazani, S. A. A.; Tavakolzadeh, F.; Baniasadi, H. Polym Compos 2009, 30, 1388.
11. Ramazani, S. A. A.; Tavakolzadeh, F.; Baniasadi, H. Appl Polym Sci 2009, 115, 308.
12. Nikkhah, S. J.; Ramazani, S. A. A.; Baniasadi, H.; Tavakolzadeh, F. Mater Des 2009, 30, 2309.
13. Baniasadi, H.; Ramazani, S. A. A.; Javan, S. Mater Des 2009, 31, 76.
14. Trujillo, M.; Arnal, M. L.; Muller, A. J. Macromolecules 2007, 40, 6268.
15. Kaminsky, W.; Funck, A.; Wiemann, K. Macromol. Symp 2006, 239, 1.
16. Zhang, W.; Shen, L.; Phang, I.; Liu, T. Macromolecules 2004, 37, 256.
17. Liu, T.; Phang, I.; Shen, L.; Chow, S.; Zhang, W. Macromolecules 2004, 37, 7214.
18. Qian, D.; Dickey, E.; Andrews, R.; Rantell, T. Appl Phys Lett 2000, 76, 2868.
19. Jin, L.; Bower, C.; Zhou, O. Appl Phys Lett 1998, 73, 119.
20. Sun, Y.; Fu, K.; Lin, Y.; Huang, W. Acc Chem Res 2002, 35, 1096.
21. Bredeau, S.; Boggioni, L.; Bertini, F.; Tritto, I.; Monteverde, F.; Alexandre, M.; Dubois, P. Macromol Rapid Commun 2007, 28, 822.
22. Kaminsky, W.; Funck, A. Macromol Symp 2007, 260, 1.
23. Sanchez, Y.; Albano, C.; Karam, A.; Perera, R.; Casas, E. Macromol Symp 2009, 282, 185.
24. Park, S.; Choi, I. S. Adv Mater 2009, 21, 902.
25. Liang, G. D.; Tjong, S. C. Mater Chem Phys 2006, 100, 132.
26. Zohuri, G.; Jamjah, R.; Mehtarani, R.; Ahmadjo, S.; Nekoomanesh, M. Iran Polym J 2003, 12, 32.
27. Kim, J. Y.; Kim, S. H. J Polym Sci Part B: Polym Phys 2006, 44, 1062.